Structural model and atomic positions

Table S1: Structural models and atomic positions for A_3C_2 systems.

Systems	a (Å)	b (Å)	c (Å)	Atomic positions
Ti_3C_2	3.099	3.099	19.318	Ti: 2i (0.667, 0.333, 0.379); Ti: 1b (0.0, 0.0, 0.5); C: 2h (0.333, 0.667, 0.569).
Zr_3C_2	3.369	3.369	20.289	Zr: 2i (0.667, 0.333, 0.369); Zr: 1b (0.0, 0.0, 0.5); C: 2h (0.333, 0.667, 0.574).
Hf_3C_2	3.317	3.317	19.859	Hf: 2i (0.667, 0.333, 0.370); Hf: 1b (0.0, 0.0, 0.5); C: 2h (0.333, 0.667, 0.569).

The Hamiltonian of the classical Heisenberg model

We performed a Monte Carlo simulation to estimate the Curie temperature of the A_3C_2 systems. The simulation is based on the Ising model.

The Hamiltonian of the classical Heisenberg model can be shown to be

$$H = -\Sigma_{i,j} J_1 N_i N_j - \Sigma_{k,l} J_2 N_k N_l \quad (1),$$

where J_1 and J_2 are the first and second nearest-neighbor exchange parameters, respectively. For A_3C_2 with the $P\bar{6}m2$ type structure, we construct a 50 × 50 supercell. J_1 and J_2 are estimated by the following formulas:

$$E(FM) = -24J_1N^2 - 4J_2N^2 \quad (2)$$

$$E(AFM1) = -24J_1N^2 + 4J_2N^2 \quad (3)$$

$$E(AFM2) = 8J_1N^2 - 4J_2N^2 \quad (4)$$

$$\Delta E_2 = E(AFM1) - E(FM) = 8J_2N^2 \quad (5)$$

$$\Delta E_1 = E(AFM2) - E(FM) = 32J_1N^2 \quad (6)$$

$$J_1 = \frac{\Delta E_1}{32N^2} \quad (7)$$

$$J_2 = \frac{\Delta E_2}{8N^2} \quad (8)$$

Table S2: Structural models, atomic positions, and total magnetism for A_3C_2 systems.

Systems	J_1 (meV)	J_2 (meV)
Ti_3C_2	14.0	21.3
Zr_3C_2	13.3	18.9
Hf_3C_2	5.5	13.4

Table S3: Curie temperature estimated by Monte Carlo simulation with different U parameters (U = 1-3 eV) for A_3C_2 systems.

T_C (K)	U = 1 eV	U = 2 eV	U =3 eV
Ti_3C_2	972	972	984
Zr_3C_2	656	652	644
Hf_3C_2	340	364	412

Table S4: Calculated total and atomic magnetic moments for A_3C_2 systems.

Systems	Total magnetic moment (μ_B)	Atomic magnetic moment （AMM） (μ_B)	AMM (μ_B)	AMM (μ_B)
Ti_3C_2	1.95	Ti (2i)：0.975	Ti (1b)：0	C (2h)：0
Zr_3C_2	1.95	Zr (2i)：0.975	Zr (1b)：0	C (2h)：0
Hf_3C_2	1.50	Hf (2i) ：0.75	Hf (1b)：0	C (2h)：0

Magnetic anisotropy energy (MAE) difference

Table S5: magnetic anisotropy energy (MAE) difference between the [100] and [001] direction for Ti_3C_2. SOC is added during the calculations.

	U = 0 eV	U = 1 eV	U = 2 eV	U =3 eV
[100]-[001]	19.6 μeV	18.7 μeV	18.5 μeV	18.3 μeV

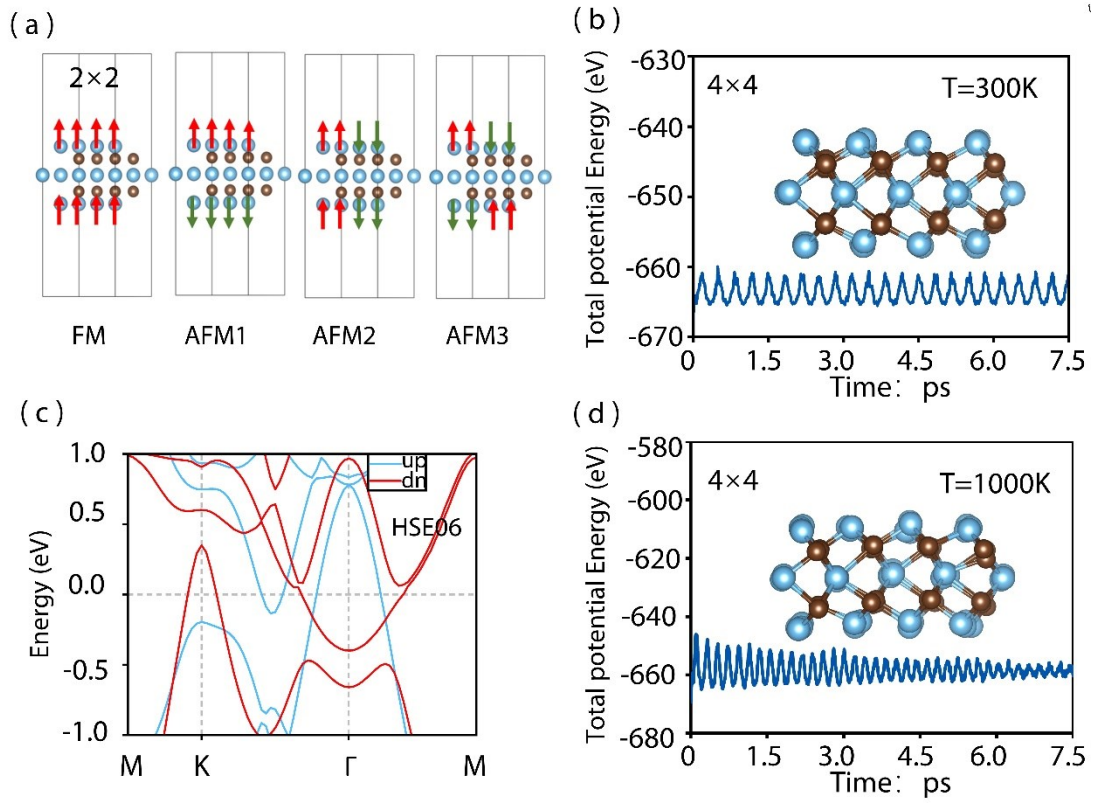

Figure S1. (a) 2×2 supercell of A_3C_2 and different magnetic states, with the arrows showing the spin direction of the A (A = Ti, Zr, and Hf) atoms; (b)/(d) the total potential energy fluctuation of Ti_3C_2 during the *ab initio* molecular dynamics (AIMD) simulation at 300 K/1000K, with the inset showing the atomic configuration of Ti_3C_2 after 7.5 ps of AIMD simulation at 300 K/1000K; (c) spin-polarized band structure of Ti_3C_2 calculated via the HSE 06 method.

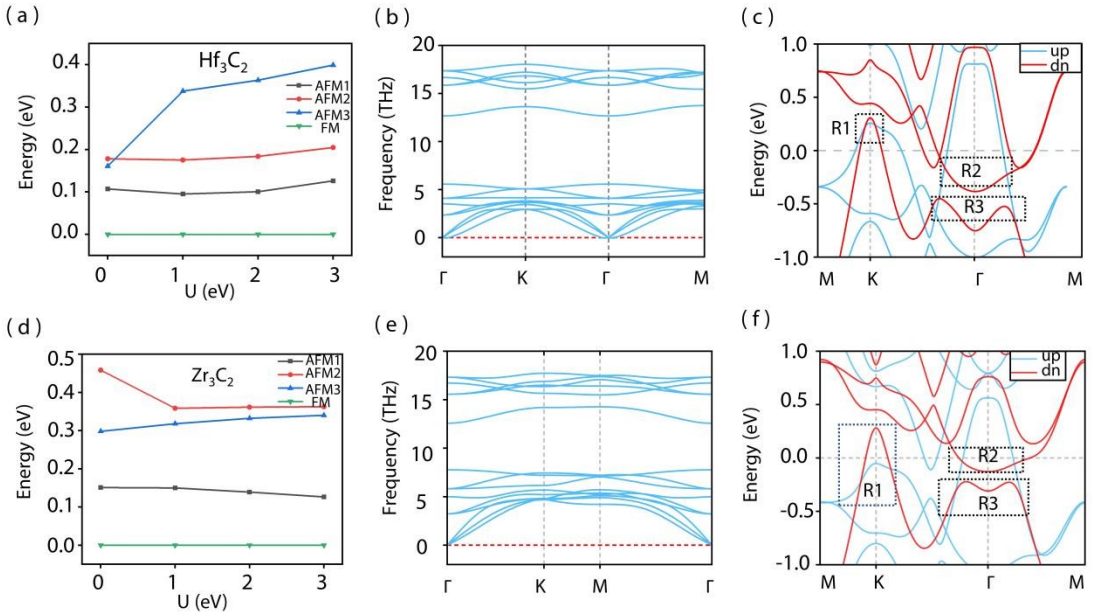

Figure S2. (a) Total energies of Hf_3C_2 in the FM and AFM1-3 magnetic states (with the energy of FM set to 0 eV); (b) calculated phonon dispersion of Hf_3C_2; (c) spin-polarized band structure of Hf_3C_2; (d) total energies of Zr_3C_2 in the FM and AFM1-3 magnetic states (with the energy of FM is set to 0 eV); (e) calculated phonon dispersion of Zr_3C_2; (f) spin-polarized band structure of Zr_3C_2.

Edge states

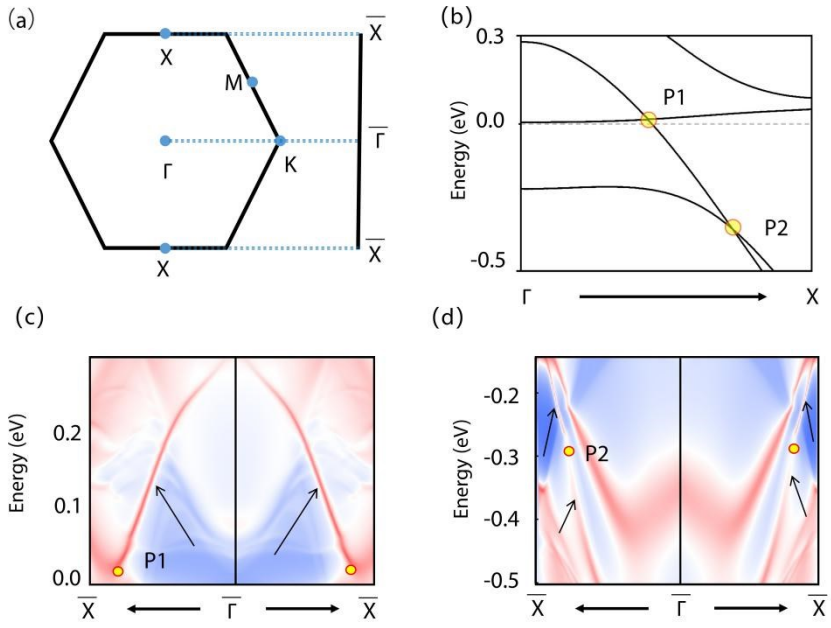

Figure S3 (a) the 2D BZ and the projection onto the (010) edge; (b) Band structures along the Γ-X; (c) and (d) The projection spectrum on the edge of (010). SOC is added during the calculations.

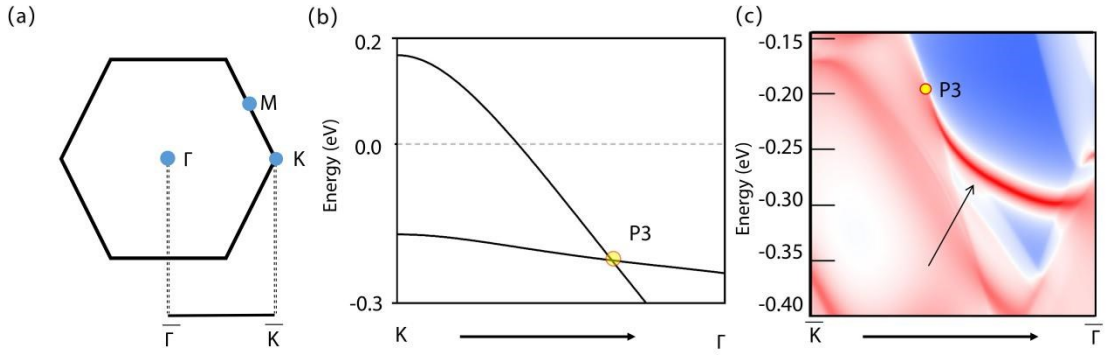

Figure S4 (a) the 2D BZ and the projection onto the (110) edge; (c) Band structures along the K-Γ path; (c) and (d) The projection spectrum on the edge of (110). SOC is added during the calculations.

In 3D nodal-line semimetals, nodal lines are characterized by nontrivial drumhead surface states. Here, we calculate the edge states for the Ti_3C_2 monolayer. The results of (010) and (110) edge are shown in Figure S3 and Figure S4, respectively. Based on the energy range of the nodal lines in Figure S3(b) and Figure S4(b), edge states in Figure S3(c), Figure S3(d) and Figure S4(c) correspond to nodal lines in R2, R3 and R1 respectively.

Types of nodal lines

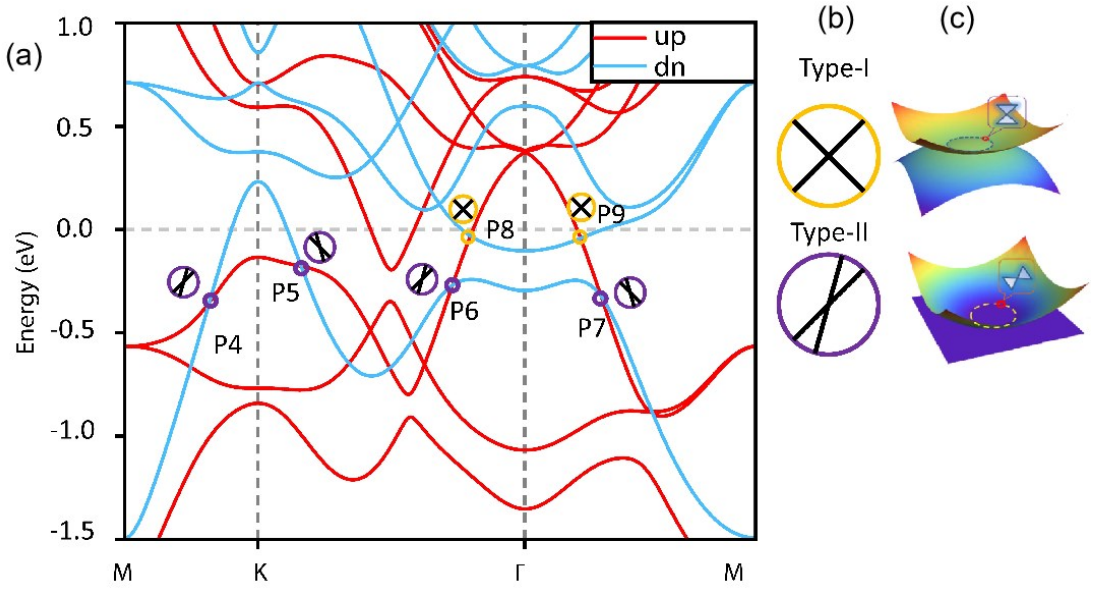

Figure S5 (a) band structures of Ti_3C_2; (b) type I and type II band crossing points are shown schematically in (b); (c) schematic figure of type I and type II nodal lines (see New J. Phys. 20 (2018) 053019).